Jiří Krýže

Methods for storage and processing of analog data, used in MUSA-6

Kybernetika, Vol. 1 (1965), No. 2, (144)--179

Persistent URL: http://dml.cz/dmlcz/125211

KYBERNETIKA ČÍSLO 2, ROČNÍK 1/1965

Methods for Storage and Processing of Analog Data, Used in MUSA-6

JIŘÍ KRÝŽE

Sampling, PDM encoding, recording, reproducing, multiplication, interpolation and summation of samples of analog signals are analysed as parts of a data processing chain and their error contribution to the total error is evaluated, when different kinds of deviations from ideal operation are assumed.

INTRODUCTION

The machine MUSA-6 is a specialized analog machine, designed mainly for statistical computation. Its memory consists of a six track magnetic tape, corresponding to six main working channels of the machine. This led to its name (Magnetic tape Universal Statistical Analyser with six channels). It was designed for the following main tasks:

1. Evaluation of autocorrelation and crosscorrelation functions.
2. Evaluation of distribution functions.
3. Evaluation of Fourier integrals.
4. Computation of convolution integrals.
5. Simulation of a time lag, which depends on some variable.
6. Formation of a memory for an analog computer.
7. Transformation of time scales of continuous processes.

The basic principles of these computations, the block structure of the machine and its use for flexible programming of various tasks were described in previous papers [14] and [15]. The scope of this paper will be concentrated to analog algorithms used for storage and processing of analog signals, used in the machine.

As the machine was intended especially for research work, the demand for accuracy was substantially more stressed than in some previous works dealing with this kind of analog computation. A machine error substantially lower than the method error was required. This consequently led to the demand for the maximum accuracy which could be achieved with the analog principle and hardware given.

The effort in developping improved techniques of analog signal storage resulted in some new analog algorithms which are much more characteristic for the machine construction than the basic computation principles, which have a great deal in common with those known from previous work.

The high demands for accuracy forced a time-discontinuous method to be chosen for tape recording.

Contrary to some previous works, where discontinuous methods of tape recording, such as frequency modulation, pulse repetition frequency modulation or pulse width modulation, were used for the same reasons, the time-discontinuous form of signals in the MUSA is not limited to the read and write circuits. It is the basic form used throughout the machine. All operations are performed on equidistant samples and the output signals are obtained by interpolating the samples of the result. In this respect there is a definite analogy with the operation of a digital computer. This gives a possibility for simple exact mathematical formulations of all machine operations. The influence of inherent frequency response limitations on the result obtained can be computed exactly and the involved errors corrected in further processing, if necessary. The fact that, at least in equidistant intervals, the output signal has practically exactly the correct value, is of importance in nearly all planned applications.

When transforming continuous signals into time-discontinuous forms, the mentioned goals cannot be achieved by using methods inherently bound to non equidistant sampling, such as the methods based on comparison of continuous signals and some coding signals (saw-tooth for instance), or frequency modulation methods. These methods are bound to filtering by complex filters. The resulting very complex mathematical relation between instantaneous imput and output signal values includes linear and non-linear error terms, which can be supressed only by frequency-band limitations. These limitations are tolerable when an accuracy in the range of 1% is acceptable, but when the total error (including noise) has to be reduced to $1^0/_{00}$, or even less, the frequency response limitations become severe in spite of the great pulse density on the tape used for frequency modulation recording. There is one further point:

For frequency modulation recording, the value of percentual speed fluctuations of the tape transport has to be substantially lower than the acceptable percentual noise and error level when not very complex correction circuitry, based on some form of clock signals on auxiliary tracks, is to be used.

This is not necessarily the case with PDM methods, as used in MUSA-6.

Therefore, the FM recording which is most frequent for analog signal recording, was abandoned and a refined PDM method used. The first step of this method is based on first sampling and then converting the equidistant samples into a duty-cycle pulse modulated signal.

SAMPLING

The sampling and holding of equidistant instantaneous values of continuous signals seems to be very simple in theory, but gives much trouble in practice, when

great accuracy and higher sampling frequencies are demanded. This means charging a capacitor in microseconds to an exact value, and holding this value exactly for a time two or three orders of magnitude greater, and making it available on a low-impedance output without the possibility of using the benefits of negative feedback from output to input.

Besides these practical difficulties, there are theoretical ones, too. The mixing action of sampling causes undesirable distortion components with frequencies lower than half the sampling frequency to appear in the sampled output signal, when frequencies

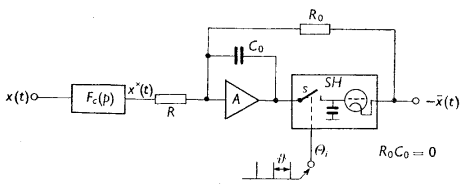

Fig. 1. Mean value sampling circuit with correction filter.

higher than half the sampling frequency are contained in the input signal. Thus, undesired high-frequency components, such as hum and noise, can affect the sampled values very substantially.

The above mentioned difficulties led to the decision to sample, instead of the instantaneous values, the mean values of the continuous signal in the respective sampling intervals. This resulted in a considerable reduction of undesired frequency components higher than the sampling frequency on the one hand, and in a possibility of using a negative feedback loop on the other hand, as shown in figure 1.

Here A is an operational amplifier, SH is a conventional sampling and holding circuit with unity gain, with an electronic switch s and a capacitor memory. (Its circuitry is, of course, much more sophisticated than the basic principle shown in SH in Fig. 1.) The time constant R_0C_0 is equal to the sampling interval ϑ and $R = R_0$. Then, by trivial analysis, it can be shown that

$$\bar{x}_i = \frac{1}{\vartheta}\int_{\Theta_{i-1}}^{\Theta_i} x^*(t)\,\mathrm{d}t\,, \tag{1}$$

where

$$\Theta_{i+1} = \Theta_i + \vartheta$$

are the sampling instants, $\bar{x}_i$ is the negative value of the sampled output $-\bar{x}(t)$ in the i-th sampling interval, beginning with Θ_i and terminating in Θ_{i+1}. It is evident that long-time drifts and non-linearities of the sampling and holding circuit behave in the same way as similar errors of the output stage of the amplifier. Their influence on the transfer of slowly varying signals can be made sufficiently small by choosing the gain of A sufficiently great. Thus, the specifications for the sampling and holding circuit

can be made much less severe. Influence of nonlinearity and gain variations of SH have to be respected only with rapidly varying signals. Denoting by a the gain of the sampling and holding circuit the equation (1) can be written in its more general form.

$$\bar{x}_{i+1} = \left(1 - \frac{a\vartheta}{R_0 C_0}\right) \bar{x}_i + \frac{a}{RC_0} \int_{\Theta_i}^{\Theta_{i+1}} x^*(t)\, \mathrm{d}t \,. \tag{2}$$

For $x^*(t) = \text{const} = x_e$ the solution is

$$\bar{x}_i = + \frac{R_0}{R} x_e \tag{3}$$

and is independent of a and C_0, as far as the difference equation (2) is stable, that is, as far as

$$\left|1 - \frac{a\vartheta}{R_0 C_0}\right| < 1 \,.$$

Deviations in the value of $a\vartheta/R_0C_0$ from 1, caused by changes in a (nonlinearity, for instance, or aging) ϑ, R_0, C_0 affect only the dynamic properties, by introducing the undesired term $\bar{x}_i$ in the difference equation (2). The consequence is a distortion of the response to an ideal step function in $x^*(t)$ (the step beginning in some Θ_i), which is in case of eq. 1 an ideal step (delayed by ϑ) too, but in case of (2) a stepwise exponential transient, damped by the coefficient $(1 - [a\vartheta/R_0C_0])$ for each step. When $|1 - (a\vartheta/R_0C_0)| < 10^{-2}$, then the error in the step value in the first sampling interval will be smaller than 1% of the step value and smaller than 0.01% in the following interval. Thus, the influence of possible imperfections in SH quality is quickly ruled out by the feedback loop.

As can be seen from the structure of the sampling circuit in Fig. 1, it answers only to mean values of $x(t)$ and $\bar{x}(t)$, and equations (1) and (2) are expressions for relations between these mean values.

Thus, if leakages in the memory condenser or other parts of the SH unit cause $\bar{x}(t)$ not to be strictly constant during one sampling interval, equations (1) and (2) still hold if $\bar{x}_i$ is taken as the mean value of $\bar{x}(t)$ in the respective sampling period.

But by taking mean value of $x^*(t)$ instead of the instantaneous value in Θ_i, the frequency response of the sampling method is greatly affected. By means of Taylor series expansions or by Fourier representation of the output it can be shown that this change is equivalent to filtering the continuous signal by a filter with a transfer function:

$$\mathrm{e}^{-\frac{1}{2}\vartheta p} \cdot \frac{2}{\vartheta p} \sinh \frac{\vartheta p}{2} \tag{4}$$

before applying it to the input of a conventional sampling circuit for instantaneous sampling.

Therefore, a correction filter with a transfer function

$$\frac{\frac{1}{2}\vartheta p}{\sinh \frac{1}{2}\vartheta p} = 1 - \frac{\vartheta^2 p^2}{24} + \frac{7\vartheta^4 p^4}{5760} + \dots \tag{5}$$

should be used for correction. The time delay $\frac{1}{2}\vartheta$ in (4) is of no importance in the applications involved. It only adds to the intentionally generated time delays which are necessary for the machine operations.

A correction filter with the transfer function (5) is not realisable because of inherent instability. Therefore, some approximation has to be tried. Taking the first two terms of the series expansion in (5) seems to be the simplest solution. However, it means introducing the second derivative, which is undesirable both from the hardware point of view and from high frequency noise considerations. Therefore, a correction filter ($F_c(p)$ in Fig. 1) formed by a simple passive RC network with a transfer function

$$F_c(p) = \frac{1 + 3\tau p}{1 + 3\tau p + \tau^2 p^2} = 1 - \frac{\vartheta^2 p^2}{24} + \dots \tag{6}$$

with

$$\tau^2 = \frac{\vartheta^2}{24}$$

was finally chosen. This filter does not stress frequencies higher than $1/\vartheta$, on the contrary, it damps them.

Thus, the resulting transfer function [valid for frequencies lower than $1/(2\vartheta)$] of the whole sampling circuit in Fig. 1, including the $\frac{1}{2}\vartheta$ delay of the holding action, is

$$F_s(p) = \frac{1 + 3\tau p}{1 + 3\tau p + \tau^2 p^2} \cdot e^{-\delta p} \cdot \frac{2}{\vartheta p} \sinh \frac{\vartheta p}{2}, \tag{7}$$

and the value of $\bar{x}_i$ is a very close approximation of the instantaneous value of $x(t)$ in the middle of the preceding sampling interval, the term $(\vartheta^2 p^2)/24$ in (5) and (6) series expansions reflecting the first-order influence of $x(t)$ waveform curvature on the difference between the mean and the mentioned instantaneous value.

The absolute value of the frequency response characteristic is

$$|F_s(j\omega)| = \frac{2}{\omega\vartheta} \sin \frac{\omega\vartheta}{2} \sqrt{\left(\frac{1 + 9\tau^2\omega^2}{1 + 7\tau^2\omega^2 + \tau^4\omega^4}\right)} = 1 - \frac{87}{5760}\omega^4\vartheta^4 + \dots$$

The amplitude characteristic, thus, remains constant to frequencies very close to the theoretical maximum $1/(2\vartheta)$.

The phase shift (without regard to the harmless fixed delay ϑ) is

$$\operatorname{tg} \chi_s = \frac{3\omega^3\tau^3}{1 + 8\omega^2\tau^2},$$

and is also harmless over a substantial part of the frequency band.

Of course, the method used does not exclude the use of better and more sophisticated correction filters, if necessary.

CODING

For the conversion of the sampled signal in a duty cycle pulse modulated signal (abreviation PDM signal), comparison with a triangular coding waveform was used (see Fig. 2). The instants of coincidence of the sampled signal $\bar{x}(t)$ and the coding

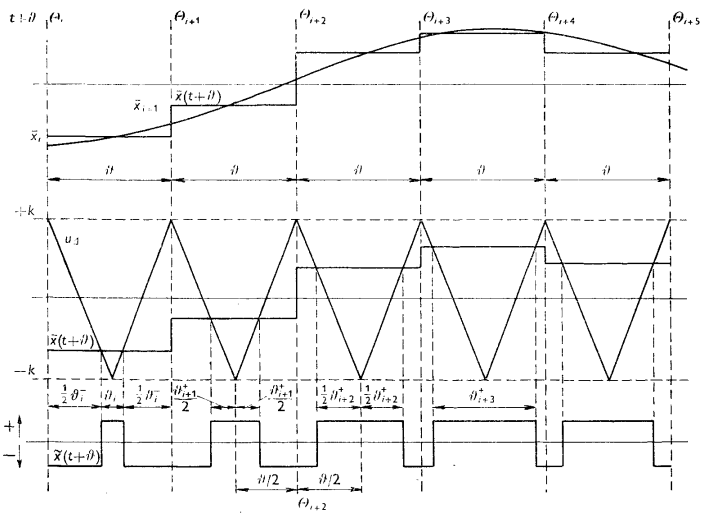

Fig. 2. Coding waveforms.

waveform u_Λ are instants of polarity changes of the PDM signal $\tilde{x}(t)$. The value $\bar{x}_i$ is represented in the i-th interval of $\tilde{x}(t)$ by the relation of the positive (ϑ_i^+) and negative (ϑ_i^-) parts of the PDM signal in the respective sampling period to the whole period ϑ:

$$\bar{x}_i = \frac{2\vartheta_i^+ - \vartheta}{\vartheta} = k\,\frac{\vartheta_i^+ - \vartheta_i^-}{\vartheta}\,. \tag{8}$$

Here k denotes the peak amplitude of u_Λ. The maximum value of $|\bar{x}_i|$ is supposed to be 1. Then $1/k$ expresses the maximum modulation depth of the PDM. Instead of the triangular waveform, a saw-tooth waveform is frequently used for similar purposes. In fact, there is little difference in principle. The triangular waveform can be dealt with

as a composition of two saw-tooth wave-forms with an opposite slope. But the inherent symmetry of the triangular waveform yields many valuable advantages, e.g.:

a) Influence of waveform distortions.

The linear parts of the triangular and saw-tooth waveforms are to be generated by integration of constant voltages. This integration is never quite ideal. Instead of the ideal integration transfer function

(9) $$\frac{1}{\tau p}$$

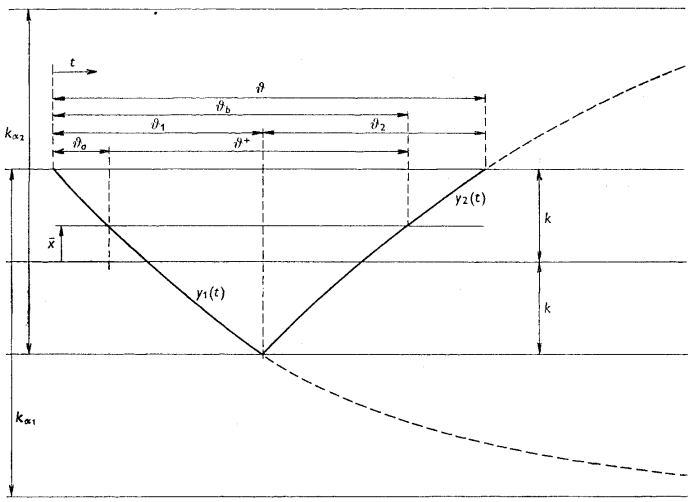

Fig. 3. A generalized exponential distorted triangular waveform.

the transfer function of the integration network is

(10) $$\frac{1}{\tau p + a}$$

or an even more complex one. Here a is due to the finite gain and pass band of the integration amplifier, or to leakage in the integration condenser, and so on. Thus the waveforms are not strictly linear, but formed by exponentials. In the case of transfer function (10) the wave forms consist of parts of two simple exponentials (see Fig. 3).

The two exponentials are characterized by their time constants τ_1 and τ_2 and their asymptotic values $k\alpha_1$ and $k\alpha_2$ respectively. The leading edge of the coding waveform is described by the equation

$$y_1(t) = k[1 - \alpha_1(1 - e^{-t/\tau_1})] \tag{11}$$

with

$$\frac{\tau_1}{\vartheta_1} = -\frac{1}{\ln(1 - 2/\alpha_1)}, \tag{12}$$

so that

$$y_1(\vartheta_1) = -k.$$

Similarly, for the trailing edge

$$y_2(t) = k[1 - \alpha_2(1 - e^{-(t-\delta_1)/\tau_2})] \tag{13}$$

with

$$\frac{\tau_2}{\vartheta_2} = -\frac{1}{\ln(1 - 2/\alpha_2)} \tag{14}$$

ϑ_a and ϑ_b are found from the conditions

$$y_1(\vartheta_a) = y_2(\vartheta_b) = \bar{x}. \tag{15}$$

Then the coding error with respect to (8) has to be defined as

$$\delta = k\frac{2\vartheta^+ - \vartheta}{\vartheta} - \bar{x} = k \cdot \frac{2(\vartheta_b - \vartheta_a) - \vartheta}{\vartheta} \tag{16}$$

and can be expressed as

$$\delta = 2k\frac{\vartheta_1}{\vartheta} - k - \bar{x} + \frac{2k\tau_1}{\vartheta}\ln\frac{k\alpha_1 - k + \bar{x}}{k\alpha_1} - \frac{2k\tau_2}{\vartheta}\ln\frac{k\alpha_2 - k - \bar{x}}{k\alpha_2}. \tag{17}$$

Using series expansions of (12), (14) and (17), valid for α_1 and α_2 sufficiently large and supressing terms of order α_1^{-4}, α_2^{-4} and lower, an approximation may be found as follows:

$$\begin{aligned}\delta \doteq k\left(1 - \frac{\bar{x}^2}{k^2}\right)\Bigg\{&\frac{\vartheta_1}{2\alpha_1\vartheta}\left(1 + \frac{1}{\alpha_1} + \frac{5}{3\alpha_1^2}\right) - \frac{\vartheta_2}{2\alpha_2\vartheta}\left(1 + \frac{1}{\alpha_2} + \frac{5}{3\alpha_2^2}\right) - \\ &- \frac{\bar{x}}{3k}\left[\frac{\vartheta_1}{\alpha_1^2\vartheta}\left(1 + \frac{2}{\alpha_1}\right) + \frac{\vartheta_2}{\alpha_2^2\vartheta}\left(1 + \frac{2}{\alpha_2}\right)\right] - \frac{1}{4}\left(1 - \frac{\bar{x}^2}{k^2}\right)\left(\frac{\vartheta_1}{\alpha_1^3\vartheta} - \frac{\vartheta_2}{\alpha_2^3\vartheta}\right)\Bigg\}.\end{aligned} \tag{18}$$

For the isosceles triangle waveform $\vartheta_1 = \vartheta_2 = \frac{1}{2}\vartheta$ and also $\tau_1 = \tau_2 = \tau$ and $\alpha_1 = \alpha_2 = \alpha$, as the same fixed parameter integration network is used, as a rule, for generating the two edges.

Then

$$\delta \doteq -\bar{x}\left(1-\frac{\bar{x}^2}{k^2}\right)\frac{1}{3\alpha^2}\left(1+\frac{2}{\alpha}\right). \tag{19}$$

Finding the maximum deviation of δ from an optimally chosen strainght line

$$\delta = \lambda\bar{x}$$

eads to the maximum nonlinearity error

$$\delta_n = \left|\delta - \lambda_{\mathrm{opt}}\bar{x}\right|_{\max} = \frac{\alpha+2}{12k^2\alpha^3}. \tag{20}$$

For a saw-tooth waveform $\vartheta_2 \ll \vartheta_1$, $\vartheta_1 \doteq \vartheta$ and α_2 cannot be smaller than 2. Thus

$$\delta \doteq \frac{k}{2\alpha_1}\left(\frac{\bar{x}^2}{k^2}-1\right) \tag{21}$$

when terms of lower order in α_1 are neglected. Then the nonlinearity error is

$$\delta_n = \frac{1}{4k\alpha_1}. \tag{22}$$

The comparison of (20) and (22) shows that the error due to finite α is much smaller in the case of an isosceles triangular waveform. For example, when $\delta_n < 10^{-4}$ is acceptable, for $k = 1{\cdot}25$, α_1 has to be larger than 2000 in the case of a saw-tooth waveform, whereas α larger than 23.8 is sufficient for a triangular voltage. When the edges of the coding voltages are generated by integration of a constant voltage $u_0 = k/\kappa$, then $\kappa(\alpha - 1)$ is the minimum necessary gain of the operational amplifier used in the integrator. The gain necessary for triangular waveforms is thus much smaller, which is of great value for higher coding waveform frequencies.

b) Influence of sampling omitted.

Fig. 4 shows the situation when an unsampled signal $x(t)$ is directly coded by means of a triangular coding waveform. When for $x(t)$ only the first two terms of its series expansion in the centre of the sampling interval are taken

$$x(t) = \bar{x}_i + x_i' \,.\, t\,, \tag{23}$$

and ϑ_i^+ is computed and the error definition (16) is applied, then

$$\delta_i = \frac{\left(1+\frac{\bar{x}_i}{k}\right)\left(\frac{\vartheta x_i'}{4k}\right)^2}{1+\left(\frac{\vartheta x_i'}{4k}\right)^2} \tag{24}$$

is obtained. This equation shows nonlinear distortions which become significant when the increment $\vartheta x'$, of $x(t)$ during one sampling interval ϑ increases. But with

such rapidly varying signals, distortions due to higher derivatives become significant, so that the limitations on signal variations imposed by omission of sampling are even stronger. Equation (24) is of great importance with respect to the necessary quality of the holding action of the sampling circuit. The leakage of the memory condenser in the SH unit in Fig. 1 causes an approximately linear variation of its output voltage during one sampling period. But the mean value of this voltage is correct. This is secured by the feedback. Equation (24) thus indicates that a rather poor holding action characterized by 10% full scale drift during one sampling period, is still acceptable.

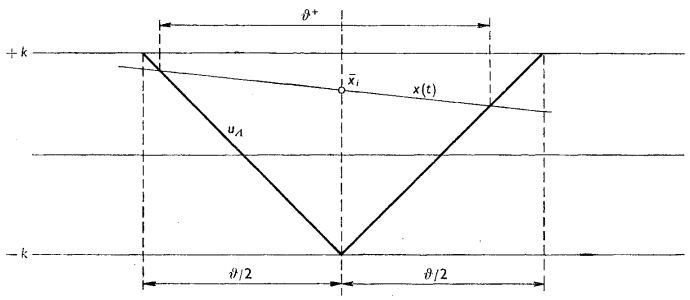

Fig. 4. Coding of nonsampled waveforms.

This is not the case with a saw-tooth coding waveform. If a falling ramp is used, the expression for δ becomes

$$\delta_i = -\frac{\vartheta x_i' \bar{x}_i}{2k + \vartheta x_i'} \tag{25}$$

and indicates a much greater error. For $\delta < 10^{-3}$ and $k = 1{\cdot}25\ \vartheta x' < 2{\cdot}5 \,.\, 10^{-3}$ is necessary.

Thus it is obvious that the inherent symmetry of an isosceles triangular coding waveform has substantial advantages when high precision is to be secured.

RECORDING

The information density on the magnetic tape, expressed in the number of samples per unit length of one track, is limited by the minimum distance of two pulses. When the tape speed v is used, the minimum distance is

$$\lambda_{\min} = v\vartheta^+_{\min} = \lambda \,.\, \frac{\vartheta^+_{\min}}{\vartheta}, \tag{26}$$

where $\lambda = v\vartheta$ is the sample distance on the tape. Evaluation of $\vartheta^+_{\min}$ from (8) for $\bar{x} = -1$ yields

$$\frac{\vartheta^+_{\min}}{\vartheta} = \left(1 - \frac{1}{k}\right) \cdot \frac{1}{2} \tag{27}$$

and

$$\lambda_{\min} = \tfrac{1}{2}\lambda\left(1 - \frac{1}{k}\right). \tag{28}$$

The equations (26), (27) and (28) are valid for both the triangular and saw-tooth coding waveforms, and so these waveforms are quite equivalent from the information density viewpoint.

From (28) it can be seen that for a given $\lambda_{\min}$ the sample distance λ is to be increased if the modulation depth $1/k$ increases. Thus a choice of a small modulation depth seems to be advantageous.

But a certain random error in the position of recorded pulses exists, due to a tape coating structure, head gap dimensions, and varying tape to head contact. As a result, the intervals ϑ_i^+ and ϑ_i^- are, after being recorded and reproduced, obtained with a random error, due to a random shift of the recorded pulses by a maximum amount $\Delta\lambda$, depending on head and tape quality. Written (8) in the form

$$\bar{x}_i = k\frac{\lambda_i^+ - \lambda_i^-}{\lambda}, \tag{29}$$

where $\lambda_i^+ = v\vartheta_i^+$ and $\lambda_i^- = v\vartheta_i^-$, permits the determination of the maximum error in $\bar{x}$ caused by $\Delta\lambda$ when it is assumed that for a given sampling interval the two polarity changes of $\tilde{x}(t)$ were shifted in opposite directions

$$\Delta\bar{x} = k\frac{(\lambda_i^+ + 2\,\Delta\lambda) - (\lambda_i^- - 2\,\Delta\lambda)}{\lambda} = k\frac{4\,\Delta\lambda}{\lambda}. \tag{30}$$

For a maximum acceptable $\Delta\bar{x}$ given, we obtain from (28) and (30)

$$\lambda \geqq 2\lambda_{\min} + \frac{4\,\Delta\lambda}{\Delta\bar{x}} \tag{31}$$

and

$$k \leqq 1 + \frac{\lambda_{\min}}{\Delta\lambda} \cdot \frac{\Delta\bar{x}}{2}. \tag{32}$$

Thus, both the values λ and k are limited through accuracy requirements and recording process qualities. $\lambda_{\min}$ has to be chosen so as to secure complete independence of adjacent pulse waveforms when reproduced. Any superposition of adjacent pulses results in a distortion of ϑ^+ and ϑ^- intervals in reading, and a nonlinearity in signal transmission is the consequence.

For MUSA-6, $\lambda_{\min} = 100\mu$ was found necessary, and it seems possible to reduce it very substantially by improving head quality which is here the main limiting factor, especially at the highest tape speed used (10 m/sec). $\Delta\lambda$ was found to lie below $0{\cdot}2\ \mu$ for an Agfa MF-3 tape, and thus for $\Delta\bar{x} < 10^{-3}$, $\lambda = 1$ mm and $k = 1{\cdot}25$ was chosen.

For a given accuracy the quantity λ and the quantity ϑ, which is to be chosen ac-

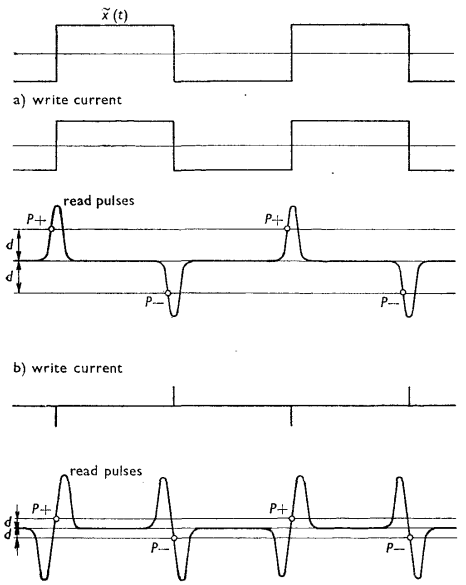

Fig. 5. PDM reading and writing methods.

cording to the spectral composition of $x(t)$, determine the necessary tape speed

$$v = \frac{\lambda}{\vartheta}. \tag{33}$$

To meet different requirements for different kinds of processes $x(t)$ and to secure economy in tape and machine time, a number of tape speeds have to be used. In MUSA-6 the speed range is from 1 mm/sec to 10 m/sec in 8 steps with a ratio of $\sqrt{10}$, and the respective range of $1/\vartheta$ from 1 c/s to 10 kc/s in similar steps.

Moreover, this enables the processing of recorded processes at a maximum speed, regardless of the speed which was used for recording.

The PDM signal $\tilde{x}(t)$ can be recorded on the tape and restored to its original form by two basic methods, both used in MUSA, and illustrated in Fig. 5. The instants of polarity changes are determined by points of the first coincidence (P_+ and P_- in Fig. 5) of the read and amplified pulses with the corresponding d level. The d levels are near zero ($\sim 5\%$ amplitude) in case b) and approximately 50% amplitude in case a). Method a) does not require erasing, but is insensitive to pulse amplitude

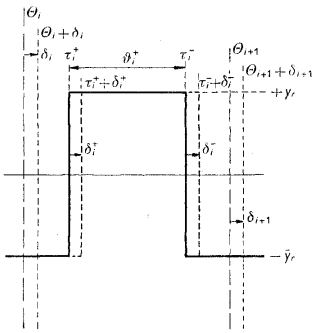

Fig. 6. Multiplicator output in one sampling interval.

variations. Method b) requires erasing, is insensitive to pulse amplitude variations, but sensitive to the noise level between pulses. Both methods can give acceptable results.

MULTIPLICATION

For multiplication the well known method of combining pulse duty modulation and amplitude modulation is used (Fig. 6). In a modulation unit the restored PDM signal $\tilde{x}(t)$ obtains in its ith inteval accurate levels $\bar{y}_r$, corresponding to the rth sampled value of a signal $y(t)$. Then, the mean value of the signal $\tilde{w}_{ir}$ obtained in this way in the ith period is, with respect to (8),

$$(\tilde{w}_{ir})_{\text{mean}} = \frac{1}{k}\,\bar{x}_i y_r\,. \tag{34}$$

The necessity of sampling the signal $y(t)$ is to be stressed. Should the sampling be omitted, (34) would change to

$$(\tilde{w}_{ir})_{\text{mean}} = \frac{1}{k}\,\bar{x}_i\bar{y}_r - y_r''\cdot\frac{\vartheta^2}{96}\left[4-\left(1+\frac{\bar{x}_i}{k}\right)^3\right], \tag{35}$$

if for $y(t)$ the first three terms of its series expansion in the centre of the sampling

interval are used:

$$y(t) = \bar{y}_r + y'_r \cdot t + y''_r \cdot \frac{t^2}{2} . \tag{36}$$

From (35) it follows that for a nonlinearity error smaller than $1‰$ of full scale ($\bar{x}_i = \bar{y}_r = 1$), the maximum deviation of $y(t)$ from an optimally chosen straight line in the given sampling period equal to $y'' \cdot (\vartheta^2/16)$, should be (for $k = 1{\cdot}25$) smaller

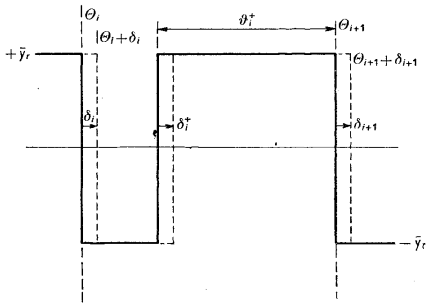

Fig. 7. Multiplicator output for saw-tooth coding.

than $1{\cdot}5 \cdot 10^{-3}$. That is a very severe limitation. On the other hand, equation (35) indicates that a linear change of $y(t)$ causes no distortion, so that slight deterioration of the holding action of the SH circuit in Fig. 1 has no effect on accuracy. This does not hold, if a saw-tooth coding voltage is used. In such case one interval of the signal $\tilde{w}(t)$ has the form indicated in Fig. 7 (for a falling ramp saw-tooth). Taking an unsampled input $y(t)$ instead of the sampled $\bar{y}_r$ then leads to a mean value

$$(\tilde{w}_{ir})_{\text{mean}} = \frac{1}{k}\bar{x}_i\bar{y}_r + \frac{\vartheta}{4}y'_r\left(1 - \frac{\bar{x}_i^2}{k^2}\right) + y''_r \cdot \frac{\vartheta^2}{24} \cdot \frac{\bar{x}^3}{k^3} \tag{37}$$

if for $y(t)$ the series approximation (36) is used.

Equation (37) indicates a large amount of nonlinear distortion due to the first derivative of $y(t)$. For $1^0/_{00}$ of full scale accuracy the change in $y(t)$ during one interval ϑ has to be below $4 \cdot 10^{-3}$.

INTERPOLATION

After multiplication, it is usually necessary to gain a smooth signal

$$w(t) = x(t - \tau)\, y(t) \tag{38}$$

or

$$w(t) = x(t - \tau) . \tag{39}$$

In the latter case $y(t) = 1$ is used. τ denotes the time lag, due to the time the tape takes to travel from one block of heads to the other. Complex low-pass filters are usually employed for attenuation of the high frequency components of $\tilde{w}(t)$ and so a smooth output waveform is obtained. The attenuation of the sampling frequency $1/\vartheta$, which is the most significant, has to be of the order of 10^3, if less than $1^0/_{00}$ ripple is required. Therefore, it is hardly possible to obtain a response time of the order $1/\vartheta$ to a step change in the $(\tilde{w}_{ir})_{\text{mean}}$ values. To overcome these limitations and

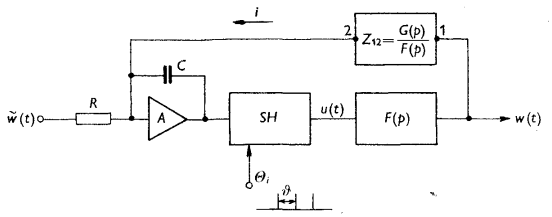

Fig. 8. Generalized interpolation circuit.

the problems of buliding very complex filters for frequencies form 1 c/s to 10 kc/s, classical filters were abandoned and discrete active filters used.

In MUSA-6, the mean value of each individual interval ϑ of $\tilde{w}(t)$ is computed and the values $(\tilde{w}_{ir})_{\text{mean}}$ so gained are interpolated parabolically. The circuit used for this purpose is based on generalization of the sampling circuit in Fig. 1. If the filter F in Fig. 1 is omitted and $\tilde{w}(t)$ used as input, then according to (2) and (34) for $(a\vartheta/RC_0) = 1$ and $R/R_0 = k$ the output of the SH circuit would be equal to $\bar{y}_i\bar{y}_r$.

Fig. 8 shows a generalization of the circuit in Fig. 1. Here $F(p)$ denotes the transfer function from u to w and $G(p)$ transfer function form u to i:

$$G(p) = \frac{i(p)}{u(p)}; \quad F(p) = \frac{w(p)}{u(p)}. \tag{40}$$

Now it can be demonstrated that it is possible to find such an $F(p)$ and $G(p)$ that the output $w(t)$ in every sampling interval is formed by a parabolic arc of the mth order traced through $m + 1$ succeeding values

$$\bar{w}_i = k(\tilde{w}_{ir})_{\text{mean}} = \bar{x}_i\bar{y}_r. \tag{41}$$

Using the discrete form of Laplace transform and designating

$$z = e^{-p\vartheta},$$

the transforms of $u(t)$ and $\bar{w}(t)$ are

$$u(z) = \sum_i u_i z^i\,, \quad w(z) = \sum_i \bar{w}_i z^i\,, \tag{42}$$

where u_i and $\bar{w}_i$ are the values of $u(t)$ and $\bar{w}(t)$ during the ith sampling interval.

Similarly, we can use the z-transform for the sequence of values $w(t)$. We define $w_i(\varepsilon)$ as

$$w_i(\varepsilon) = w(\Theta_i + \varepsilon\vartheta)\,, \quad 0 \leqq \varepsilon \leqq 1\,, \tag{43}$$

that is, the value of $w(t)$ taken in the ith interval in an instant $\varepsilon\vartheta$ after the corresponding sampling instant. Then

$$w(\varepsilon, z) = \sum_i w_i(\varepsilon)\, z^i\,. \tag{44}$$

The desired interpolation law may be expressed in a general form

$$w(\varepsilon, z) = z^\nu \bar{w}(z) \sum_{i=0}^{m} \frac{(\varepsilon + \lambda)!}{(\varepsilon + \lambda - m - 1)!\,(\varepsilon + \lambda - i)} \cdot \frac{(-z)^{m-i}}{m!} \binom{m}{i}\,. \tag{45}$$

The value of the coefficient with $z^{m+\nu-i}$ in (45) is 1 for $\varepsilon = -\lambda + i$ and zero for $\varepsilon = -\lambda + k$; $k = 0, 1, \ldots, m$; $k \neq i$. Therefore, when ε goes successively through the values $-\lambda, -\lambda + 1, \ldots, -\lambda + m$; $w(\varepsilon, z)$ goes through the values $\bar{w}(z)\, z^{m+\nu}$, $\bar{w}(z)\, z^{m+\nu-i}, \ldots, \bar{w}(z)\, z^\nu$, that is, $w_i(\varepsilon)$ goes through the values $\bar{w}_{i-m-\nu}$, $\bar{w}_{i+m-\nu+1}, \ldots, \ldots, w_{i+\nu}$. The polynomials with $z^{m+\nu-i}$ in (45) are of the order m; thus (45) is an equation of an interpolation parabola of mth order, determined by $m + 1$ succeding points of $\bar{w}_i$. Of course, only the parabolic arc for $0 \leqq \varepsilon \leqq 1$ actually appears in the output signal $w(t)$.

The waveforms of $w(t)$ are generated from $u(t)$ by means of the transfer function $F(p)$. $u(t)$ is constant during one sampling interval, and suffers sudden changes only in the sampling instants. The waveforms of $w(t)$ during one sampling interval are purely parabolical; so it is evident that they are generated by simple integrations:

$$F(p) = \sum_{n=0}^{n+m} \frac{\alpha_n}{\vartheta^n p^n}\,. \tag{46}$$

From this it follows that there will be no change in the polynomial describing $w(t)$, if there is no change in $u(t)$. That is, the polynomial valid for the ith interval would give the same values, as an extrapolation of the polynomial for the $(i-1)$th interval, if $u_i = u_{i-1}$. This can be expressed by

$$w(\varepsilon, z) = z\, w(\varepsilon + 1, z)\,. \tag{47}$$

Thus the difference

$$w(\varepsilon, z) - z\, w(\varepsilon + 1, z) \tag{48}$$

is the response of $F(p)$ to a step

$$\Delta u_i = u_i - u_{i-1}$$

or

$$\Delta\, u(z) = (1 - z)\, u(z) \tag{49}$$

in z-transform. Evaluating (48) from (45) yields

$$w(\varepsilon, z) - z\, w(\varepsilon + 1, z) = z^r \bar{w}(z) \binom{\varepsilon + \lambda}{m} (1 - z)^{m+1}\,. \tag{50}$$

Comparing (49) and (50) shows that only if

$$u(z) = A\, \bar{w}(z)\, (1 - z)^m\, z^\nu \tag{51}$$

(50) has a form

$$w(\varepsilon, z) - z\, w(\varepsilon + 1, z) = \frac{1}{A}\, \Delta\, u(z) \binom{\varepsilon + \lambda}{m}, \tag{52}$$

which can be understood as a response to a unit step $\Delta\, u(z)$ generated by a transfer function of the form (46), where

$$\alpha_n = \frac{1}{A}\left[\left(\frac{\mathrm{d}}{\mathrm{d}\varepsilon}\right)^n \binom{\varepsilon + \lambda}{m}\right]_{\varepsilon=0}. \tag{53}$$

Thus, for an interpolation of mth order, $G(p)$ has to be chosen in order to secure the appearance of mth difference of the input values on the output of the sampling unit, and $F(p)$ has to be chosen according to (46) and (53).

Denoting by $\bar{\imath}_i$ the mean value of $i(t)$ taken on the ith sampling interval, we can form the z-transform

$$\bar{\imath}(z) = \sum_i \bar{\imath}_i z^i\,. \tag{54}$$

The dependance of the values $\bar{\imath}_i$ on the values u_i can be expressed in terms of a z-transform transfer function $\varphi(z)$

$$\bar{\imath}(z) = u(z)\, \varphi(z)\,, \tag{55}$$

$\varphi(z)$ being fully determined by the choice of $G(p)$.

The basic equation of the feedback loop of Fig. 8 then follows as

$$u_{i+1} = u_i - \frac{1}{C}\int\left(i(t) + \tilde{w}(t)\,.\,\frac{1}{R}\right)\mathrm{d}t = u_i - \frac{\vartheta}{kRC}\,\bar{w}_i - \frac{\vartheta}{C}\,\bar{\imath}_i\,. \tag{56}$$

Putting

$$A = \frac{\vartheta}{kRC}\,, \tag{57}$$

forming the z-transform of (56) by using (55) leads to

$$u(z) = z\,u(z) - zA\,\bar{w}(z) - \frac{\vartheta}{C}\,z\,u(z)\,\varphi(z)$$

or to

$$u(z) = \frac{A\,\bar{w}(z)}{1 - z + \frac{\vartheta}{C}\,z\,\varphi(z)} \,. \tag{58}$$

According to (51) we need

$$u(z) = Az^{\nu}(1 - z)^{m}\,\bar{w}(z)\,,$$

so that $\varphi(z)$ has to be chosen according to

$$\frac{\vartheta}{C}\,\varphi(z) = \frac{1 - z^{\nu-1}(1 - z)^{m+1}}{z^{\nu}(1 - z)^{m}} \,. \tag{59}$$

Because of the term z^{ν} in the denomitator such a transfer function is realizable only for $\nu = 1$:

$$\frac{\vartheta}{C}\,\varphi(z) = \frac{1 - (1 - z)^{m+1}}{(1 - z)^{m}} = \sum_{n=0}^{n=m} \frac{1}{(1 - z)^{n}} \,. \tag{60}$$

Let us form a transfer function

$$G_n(p) = \vartheta p \sum_{k=1}^{k+n} \frac{1}{(\vartheta p)^k} \left[\left(\frac{\mathrm{d}}{\mathrm{d}\varepsilon} \right)^k \binom{\varepsilon + n - 1}{n} \right]_{\varepsilon = 0} \,. \tag{61}$$

The response of such a transfer function to a unit step will be

$$G_n(t) = \vartheta \frac{\mathrm{d}}{\mathrm{d}t} \left\{ \sum_{k=1}^{k=n} \frac{1}{k!} \left(\frac{t}{\vartheta} \right)^k \left[\left(\frac{\mathrm{d}}{\mathrm{d}\varepsilon} \right)^k \binom{\varepsilon + n - 1}{n} \right]_{\varepsilon = 0} \right\} . \tag{62}$$

The sum in (62) is evidently a series expansion of the function

$$\binom{\frac{t}{\vartheta} + n - 1}{n} \tag{63}$$

and thus

$$G_n(t) = \vartheta \frac{\mathrm{d}}{\mathrm{d}t} \binom{\frac{t}{\vartheta} + n - 1}{n} \,. \tag{64}$$

The mean value of $G_n(t)$ taken over the interval

$$i\vartheta \leqq t \leqq (i + 1)\vartheta$$

will be

$$\bar{G}_{ni} = \frac{1}{\vartheta}\int_{i\delta}^{(i+1)\delta} G_n(t)\,\mathrm{d}t = \binom{i+n-1}{n-1} = (-1)^i \binom{-n}{i}, \tag{65}$$

and forming the z-transform of the sequence

$$\bar{G}_n(z) = \sum_i \bar{G}_{ni} z^i = \frac{1}{(1-z)^n}. \tag{66}$$

The z-transform of a unit step is $1/(1-z)$; therefore z-transform of the response $\bar{\imath}(z)$ to a unit step in $u(z)$ according to (60) is:

$$\bar{\imath}(z) = u(z)\,\varphi(z) = \frac{C}{\vartheta}\sum_{n=0}^{n=m} \frac{1}{(1-z)^{n+1}}. \tag{67}$$

Comparison of (66) and (67) indicates that

$$G(p) = \frac{C}{\vartheta}\sum_{n=0}^{n=m} G_{n+1}(p) = \frac{C}{\vartheta}\sum_{n=0}^{k=m} \frac{\beta_k}{\vartheta^k p^k}, \tag{68}$$

where

$$\beta_k = \left[\left(\frac{\mathrm{d}}{\mathrm{d}\varepsilon}\right)^{k+1} \sum_{n=0}^{n=m} \binom{\varepsilon+n}{n+1}\right]_{\varepsilon=0}. \tag{69}$$

Both $F(p)$ and $G(p)$ are thus known for a given choice of m, λ, A, ϑ and C. The values of A and C are to be chosen from signal level considerations. The parameter λ determines the position of the actually used section of the interpolating parabola with respect to the determining set of $(m+1)$ points $\bar{w}_{i-m-\nu}, \ldots, \bar{w}_{i-\nu}$. The corresponding set of values ε is $-\lambda, \ldots, -\lambda + m$. Best interpolation results are obtained in the central interval, that is for

$$-\frac{1}{2} + \frac{m-2\lambda}{2} \leqq \varepsilon \leqq \frac{1}{2} + \frac{m-2\lambda}{2}. \tag{70}$$

If we choose this central interval as the actually used one

$$0 \leqq \varepsilon \leqq 1$$

it is evident that

$$\lambda = \frac{m-1}{2} \tag{71}$$

is necessary.

The interpolation is bound to an inherent delay. Putting in (45)

$$\varepsilon = -\lambda + i$$

yields

$$w(\varepsilon, z) = \bar{w}(z)\, z^{m+\nu-i}. \tag{72}$$

Thus, $w(t)$ goes, for $t = \Theta_k + \varepsilon\vartheta$, through the value $\overline{w}_{k-m-v+i}$ which appeared on the input in the interval from $\Theta_k - (m + v - i)\,\vartheta$ to $\Theta_k - (m + v - i - 1)\,\vartheta$. Taking the mean of these two values, we obtain the delay

$$\tau_d = (\varepsilon + m + v - i - \tfrac{1}{2})\,\vartheta = (m + v - \lambda - \tfrac{1}{2})\,\vartheta = (m - \lambda + \tfrac{1}{2})\,\vartheta\,. \tag{73}$$

For a symmetric interpolation according to (71)

$$\tau_d = \left(\frac{m}{2} + 1\right)\vartheta\,. \tag{74}$$

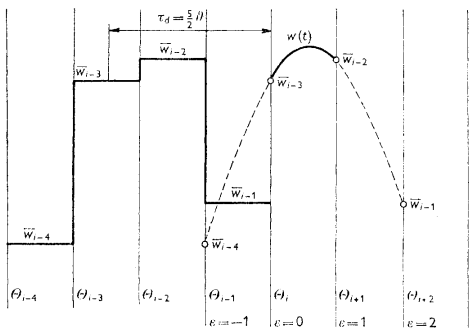

Fig. 9. Forming the interpolating output waveform in the i-ith sampling interval for a symmetric cubic interpolation.

This delay is of no principal importance in the applications in MUSA-6, as it only adds to intentionally created delays.

As an example we can take a symmetric cubic interpolation (Fig. 9) characterized by $m = 3$, $\lambda = 1$. Choosing $A = 1$ and designating

$$\frac{\vartheta}{C} = R_0 \tag{75}$$

(57) yields

$$R = \frac{R_0}{k}\,.$$

Further, in (53)

$$\binom{\varepsilon + \lambda}{m} = \tfrac{1}{6}(\varepsilon + 1)\,\varepsilon(\varepsilon - 1) = \tfrac{1}{6}\varepsilon^3 - \tfrac{1}{6}\varepsilon$$

and thus

$$\alpha_0 = 0\,, \quad \alpha_1 = -\tfrac{1}{6}\,, \quad \alpha_2 = 0\,, \quad \alpha_3 = 1\,,$$

and

$$F(p) = \frac{1}{\vartheta^3 p^3} - \frac{1}{6\vartheta p}\,.$$

In (69)

$$\sum_{n=0}^{n=m} \binom{\varepsilon + n}{n+1} = \frac{1}{24}(\varepsilon^4 + 10\varepsilon^3 + 35\varepsilon^2 + 50\varepsilon)$$

and thus

$$\beta_0 = \tfrac{25}{12}\,, \quad \beta_1 = \tfrac{35}{12}\,, \quad \beta_2 = \tfrac{2}{5}\,, \quad \beta_3 = 1\,,$$

and

$$R_0\, G(p) = \frac{1}{\vartheta^3 p^3} + \frac{5}{2}\frac{1}{\vartheta^2 p^2} + \frac{35}{12}\frac{1}{\vartheta p} + \frac{25}{12}\,.$$

The delay according to (74) is

$$\tau_d = \tfrac{3}{2}\vartheta\,.$$

The interpolation used in MUSA at present is a quadratic nonsymmetrical one (Fig. 10). A compromise with hardware considerations led to this decision. It is characterized by

$$m = 2\,, \quad \lambda = 1\,, \quad A = 1\,;$$

$$F(p) = \frac{1}{p^2} + \frac{1}{2p}\,; \quad R_0\, G(p) = \frac{1}{p^2} + \frac{2}{p} + \frac{11}{6}\,;$$

$$\tau_d = \tfrac{5}{2}\lambda\,.$$

The practical circuit shown in Fig. 11 differs from Fig. 8 in that the feedback is not taken only from output. But this is of no principal importance, if the correct transfer from $u(t)$ to input is secured. It has only to be noted that it is necessary to have some galvanic connection from output to input, otherwise the integrators involved in synthetizing $F(p)$ would cause a great output drift. If this galvanic feedback is used, the output drift is determined only by R and R_0 values and the input drift of the input amplifier. It can be seen from Fig. 11 that to change ϑ requires only to change three capacities. This is of great practical importance, when a large set of ϑ values has to be used, as it is in the case of MUSA. A detailed analysis shows that it is possible to synthetize interpolators for 3rd and 4th order interpolation with the same number of amplifiers, as in Fig. 11. The number of necessary resistors and capacitors increases, of course.

One of the simplest connections for 3rd order symmetric interpolation is shown in Fig. 12.

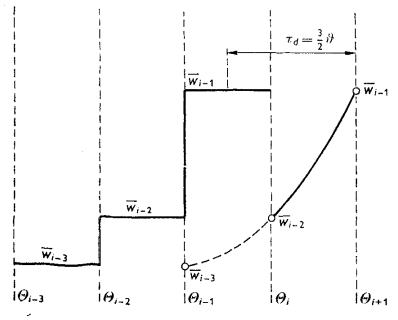

Fig. 10. Forming the interpolator output waveform in the i-ith sampling interval for a asymmetric quadratic interpolation.

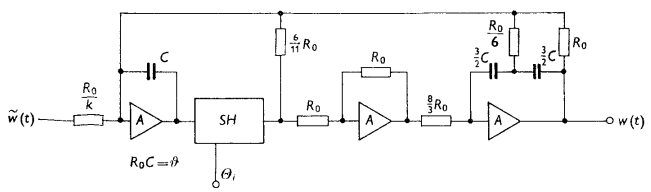

Fig. 11. Quadratic interpolation circuitry.

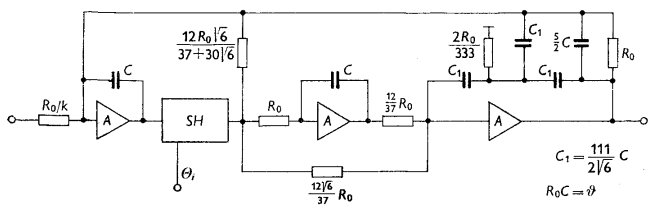

Fig. 12. Cubic interpolation circuitry.

The quality of interpolation may be judged in terms of a frequency characteristic or transfer function, valid for frequencies lower than half the sampling frequency $1/\vartheta$. From this standpoint, we see that from a sequence of discrete input values $\overline{w}_i$ (which may be dealt with as a sequence of Dirac pulses centered in their intervals) at first the

signal $u(t)$ is formed, which consists of rectangular pulses with amplitudes determined by (51). Thus the equivalent transfer function will be

$$Az(1-z)^m \frac{1-\mathrm{e}^{-\vartheta p}}{\vartheta p} \mathrm{e}^{\vartheta p/2} = A\mathrm{e}^{-\vartheta p/2} \cdot \frac{1}{\vartheta p}(1-\mathrm{e}^{-\vartheta p})^{m+1} =$$

$$= A \cdot \frac{2^{m+1}}{\vartheta p} \mathrm{e}^{-(m+2)\vartheta p/2} \sinh^{m+1} \frac{\vartheta p}{2}. \tag{76}$$

Then the signal $u(t)$ is passed through the filter $F(p)$ and so the total interpolation transfer function becomes

$$F_{I(p)} = A\left(\frac{2}{\vartheta p} \sinh \frac{\vartheta p}{2}\right) F(p) (\vartheta p)^m \mathrm{e}^{-(m+2)\vartheta p/2}$$

or

$$F_I(p) = \mathrm{e}^{-(m+2)\vartheta p/2} \left(\frac{2}{\vartheta p} \sinh \frac{\vartheta p}{2}\right)^{m+1} \sum_{k=0}^{k=m} \vartheta^k p^k \left[\left(\frac{\mathrm{d}}{\mathrm{d}\varepsilon}\right)^{m-k} \binom{\varepsilon+\lambda}{m}\right]_{\varepsilon=0}. \tag{77}$$

It may be noticed that for a symmetrical interpolation $\lambda = (m-1)/2$ the polynomial in ε is even for an even m and odd for an odd m, so that the sum in (77) is always even in p. Hence, all the phase shift in $F_I(p)$ is due to the delay $\tau_d = (m+2)\vartheta p/2$ To better see the influence of raising the frequency, it is convenient to expand

$$\mathrm{e}^{-\mathrm{j}\omega\tau_d} F_I(\mathrm{j}\omega) = 1 + \sum_{k=1}^{\infty} \alpha_k (\vartheta\omega)^{2k}. \tag{78}$$

A detailed analysis, not given here, indicates that for $\lambda = (m-1)/2$

$$\alpha_k = 0$$

for $k \leqq \frac{1}{2}m$. Thus, a higher interpolation order allows the transfer of higher frequencies for a given decrease or overshoot in amplitude. But this gain in the pass-band is rather small for $m > 4$, because for the sampling frequency

$$\omega = \frac{2\pi}{\vartheta}, \quad F_I(\mathrm{j}\omega)$$

always goes through zero.

If the interpolated output $w(t)$ is to be used for multiplication (e.g. if a correlation is being computed) it has to be sampled in coincidence with the sampling instants of the PDM input of the multiplicator.

Therefore, it is interesting to know the exact formulation of the signal transfer from interpolation input to sampling output.

The situation is as in Fig. 13 where S denotes the mean value sampling circuit (Fig. 1) and $F_c(p)$ the correction filter used with it.

Putting

$$F_c(p) = \frac{M(p)}{N(p)} = \sum_k \frac{a_k}{1 + \tau_k p} \tag{79}$$

with

$$a_k = \tau_k \frac{M\left(-\frac{1}{\tau_k}\right)}{N'\left(-\frac{1}{\tau_k}\right)}, \quad F_c(0) = 1, \tag{80}$$

and assuming that the sampling instants of $\bar{y}(t)$ are shifted with respect to the sampling instants of $\bar{w}(t)$ by an amount $\varepsilon\vartheta$, $0 \leqq \varepsilon \leqq 1$, we can, after a somewhat tedious

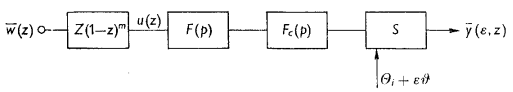

Fig. 13. Interpolation and resampling transfer functions.

calculation, not given here, express the values $\bar{y}_i$ as a linear function of the values $\bar{w}_i$. In z-transform we get

$$\bar{y}(\varepsilon, z) = z\,\bar{w}(z)\left\{z\psi^{(-1)}_{m,\lambda}(1, z) + (1 - z)^{m+2} \sum_k \frac{A_k \varrho_k^{\varepsilon}}{1 - \varrho_k z} + \right.$$

$$\left. + (1 - z) \sum_{k=-1}^{k=m} \frac{\psi^{(k)}_{m,\lambda}(\varepsilon, z)\, F_c(0)^{(k+1)}}{(k+1)!\, \vartheta^{k+1}}\right\}, \tag{81}$$

where

$$A_k = \frac{\tau_k}{\vartheta} a_k [F(p)]_{p=-1/\tau_k}; \quad \varrho_k = \mathrm{e}^{-(\tau_k/\delta)}; \quad F_c(0)^{(k+1)} = \left[\left(\frac{\mathrm{d}}{\mathrm{d}p}\right)^{k+1} F_c(p)\right]_{p=0},$$

and $\psi_{m,\lambda}(\varepsilon, z)$ is the interpolation polynomial used, known from (45):

$$\psi_{m,\lambda}(\varepsilon, z) = \sum_{k=0}^{k=m} \frac{(\varepsilon + \lambda)!}{(\varepsilon + \lambda - m - 1)!\,(\varepsilon + \lambda - k)} \binom{m}{k} \frac{(-z)^{m-k}}{m!} =$$

$$= \sum_{k=0}^{k=m} \binom{\varepsilon + \lambda - m + k - 1}{k} (1 - z)^k;$$

$$\psi^{(k)}_{m,\lambda}(\varepsilon, z) = \left(\frac{\mathrm{d}}{\mathrm{d}\varepsilon}\right)^k \psi_{m,\lambda}(\varepsilon, z); \quad \psi^{(-1)}_{m,\lambda}(\varepsilon, z) = \int_0^{\varepsilon} \psi_{m,\lambda}(\varepsilon, z)\,\mathrm{d}\varepsilon;$$

$$\psi^{(-1)}_{m,\lambda}(1, z) = [\psi^{(-1)}(\varepsilon, z)]_{\varepsilon=1}. \tag{82}$$

Equation (81) may be written also:

$$\bar{y}(\varepsilon, z) = z\,\bar{w}(z)[\psi_{m+1,\lambda+\frac{1}{2}}(\varepsilon, z) + P(\varepsilon, z) + Q(\varepsilon, z)] = \bar{w}(z)\,L(\varepsilon, z) \tag{83}$$

with

$$P(\varepsilon, z) = (1 - z)^{m+2} \sum_k \frac{A_k \varrho_k^\varepsilon}{1 - \varrho_k z} + (1 - z)^{m+1} \left[\sum_{k=0}^{k=m} \frac{1}{\vartheta^{k+1}} \binom{\lambda}{m}^{(k)} \frac{F_{\mathrm{CID}}^{(k+1)}(0)}{(k+1)!} - \right.$$

$$\left. - \binom{\lambda + \frac{1}{2}}{m+1} \right], \tag{84}$$

where

$$F_{\mathrm{CID}}(p) = \frac{\vartheta p/2}{\sinh \frac{\vartheta p}{2}}$$

is the ideal correction filter transfer function, and

$$F_{\mathrm{CID}}^{(k+1)}(0) = \left[\left(\frac{\mathrm{d}}{\mathrm{d}p} \right)^{k+1} F_{\mathrm{CID}}(p) \right]_{p=0}; \quad \binom{\lambda}{m}^{(k)} = \left(\frac{\mathrm{d}}{\mathrm{d}\lambda} \right)^k \binom{\lambda}{m},$$

and finally

$$Q(\varepsilon, z) = (1 - z) \sum \frac{\psi_{m,\lambda}^{(k)}(\varepsilon, z)}{(k+1)!\,\vartheta^{k+1}} (F_c^{(k+1)}(0) - F_{\mathrm{CID}}^{(k+1)}(0)). \tag{85}$$

Equation (83) shows that the sampled $\bar{y}(t)$ corresponds to ideal samples of a signal, gained by interpolating the $\bar{w}_i$ values by an interpolation polynomial of the order of $(m + 1)$, with λ increased by $\frac{1}{2}$ and by adding the correction terms P and Q. It has to be noted that $\psi_{m+1,\lambda+\frac{1}{2}}$ corresponds to a symmetrical interpolation if $\psi_{m,\lambda}$ is a symmetrical one.

The term P corresponds to transients, due to discontinuities of $w(t)$ and its derivatives in sampling points. These transients, as can be seen from (83), are of a form of steps with exponential fronts, occuring in sampling points ($\varepsilon = 0$, $\varepsilon = 1$). The amplitudes of these steps are proportional to the $(m + 2)$-nd difference of $\bar{w}_i$. if w_i. The term Q is due to the non-ideal transfer fuction of the correction filter used. From (85) and (82) it can be seen that this term is proportional to $(1 - z)^r$ if

$$F_c^{(k)}(0) - F_{\mathrm{CID}}^{(k)}(0) = 0 \tag{86}$$

for $k \leqq r$. Thus, if $\bar{w}_i$ has not great high order difference values, P and Q can be neglected. For the interpolation method and correction filter (given by (6)) used in MUSA

$$P(\varepsilon,z) = \tfrac{1}{24}(1 - z)^3 + (1 - z)^4 \left[\frac{A_1 \varrho_1^\varepsilon}{1 - \varrho_1 z} + \frac{A_2 \varrho_2^\varepsilon}{1 - \varrho_2 z} \right] \tag{87}$$

with

$$A_1 = -0{\cdot}00168\,; \quad A_2 = -0{\cdot}003\,; \quad \varrho_1 = 0{\cdot}154\,; \quad \varrho_2 = 2{\cdot}77\,.\,10^{-6}\,,$$

and

$$Q(\varepsilon,z) = \tfrac{1}{24}\sqrt{(\tfrac{3}{8})}\,(1-z)^3\,.$$

Defining by

$$R(k\vartheta) = \sum_i {}^1\bar{w}_i\,{}^2\bar{w}_{i-k}\,, \tag{88}$$

k being an integer, a correlation function computed from the discrete values ${}^1\bar{w}_i$ and ${}^2\bar{w}_i$, and using for ${}^1\bar{w}_i$, ${}^2\bar{w}_i$, $R(k\vartheta)$ the z-transform

$$R(z) = {}^1\bar{w}(z^{-1})\,{}^2\bar{w}(z), \tag{89}$$

we find that a value of the correlation function, computed for a shift $(k+\varepsilon)\,\vartheta$ by means of $\bar{y}(t)$, gained by interpolating and resampling the values of ${}^2\bar{w}_i$ according to Fig. 13 that

$$R(\varepsilon, z) = {}^1\bar{w}(z^{-1})\,\bar{y}(\varepsilon, z) = R(z)\,.\,\frac{\bar{y}(\varepsilon, z)}{{}^2\bar{w}(z)} = R(z)\,L(\varepsilon, z)\,. \tag{90}$$

Thus, a value of a correlation function computed for a shift $(k+\varepsilon)\,\vartheta$ follows from (81) or (83) as a linear combination of the neighbouring values $R(k\vartheta)$ and, as (83) shows, this linear combination is equivalent to a $(m+1)$-order interpolation of these values if high order differences of $R(k\vartheta)$ are small enough, as is usually the case with smooth correlation functions.

Therefore, the position of the points $R(\tau)$, for which the correlation function is actually computed, with respect to the "sampling point values" $R(k\vartheta)$, has only a negligible influence on the result. This simplifies the technical problems bound with the automatic setting of τ substantially.

INTEGRATION

In most applications of MUSA, an integral of the multiplicator output is necessary. For instance, for correlation computations, an output

$$W_i = \frac{1}{T}\int_{t_i}^{t_{i+1}} \bar{w}(t)\,\mathrm{d}t = \frac{1}{T}\int_{t_i}^{t_{i+1}} \bar{x}(t)\,\bar{y}(t-\tau_i)\,\mathrm{d}t\,, \tag{91}$$

$$t_{i+1} = t_i + T, \quad \tau_{i+1} = \tau_i + \Delta\tau$$

is required.

The machine operation is organised in such a way that the integration intervals are equidistant. (The tape is closed in an endless loop, maximum 200 m in length, and T equals one revolution of this loop.)

Then it is obvious that the mean value sampling circuit or any described interpolation circuit can be used for gaining the W_i values when ϑ is set equal to T and the

synchronizing Θ_i pulses to the SH unit are replaced by t_i pulses, gained from auxiliary tracks.

The practical circuit used in MUSA is shown in Fig. 14. It allows for zero order (for digital voltmeter output) or first order (for graphical record) interpolation of the computed values. The change of the interpolation block from Fig. 11 connection to

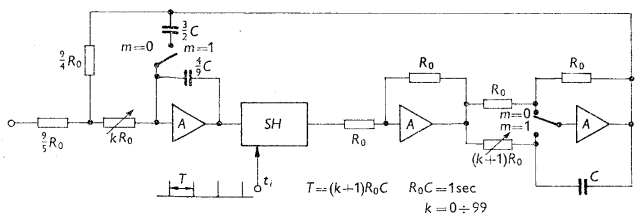

Fig. 14. Zero and first order interpolation circuitry for integral evaluation.

Fig. 14 connection is accomplished by replacing a plug-in unit. The time T is set by means of decade resistors kR_0 in steps of 2 msec in the range $1 \div 100$ sec.

SYNCHRONISATION

As can be seen from the above, to restore the PDM signals by interpolation knowledge of the sampling instants Θ_i is necessary.

For this purpose the relative position of Θ_i with respect to the moment of polarity changes of $\tilde{x}(t)$, is used.

Denoting the moment of the positive and negative polarity changes in the i-th interval by τ_i^+ and τ_i^- respectively, we can see from Fig. 2 that

$$\Theta_i = \frac{\tau_i + \tau_{i-1}}{2}, \tag{92}$$

where

$$\tau_i = \frac{\tau_i^+ + \tau_i^-}{2}. \tag{93}$$

Thus, we are able to derive the Θ_i moments from measured τ_i values. Of course, only past values can be used in defining the Θ_i in question. The simplest algorithm would be as follows:

$$\Theta_{i+1} = \frac{\tau_i + \tau_{i-1}}{2} + \vartheta. \tag{94}$$

But more sophisticated algorithms are required in practice. The main factors to be respected here are disturbances in the tape velocity which cause undesired noise in

the reproduced signal. This noise can be held to an acceptable level not only by mechanical means, which are very bulky and expensive, but by an appropriate choice of the synchronisation algorithm, too.

For this purpose, let us suppose a sinusoidal disturbance of tape velocity, which causes a time shift Δt in reproducing a pulse which otherwise would occur in a correct time interval t

$$\Delta t = a\vartheta \sin(\omega t + \varphi) = \sigma(t) . \tag{95}$$

From (8) we find

$$\tau_i^+ = \Theta_i + \frac{\vartheta}{2} - \frac{\vartheta}{4}\left(1 + \frac{\bar{x}_i}{k}\right); \quad \tau_i^- = \Theta_i + \frac{\vartheta}{2} + \frac{\vartheta}{4}\left(1 + \frac{\bar{x}_i}{k}\right). \tag{96}$$

Designating the corresponding time shifts by δ_i^+ and δ_i^- we find for $\Theta_i = i\vartheta$

$$\begin{aligned} \delta_i^+ &= a\vartheta \sin(\omega\tau_i^+ + \varphi) = a\vartheta \sin(\varepsilon_i - \lambda_i) , \\ \delta_i^- &= a\vartheta \sin(\omega\tau_i^- + \varphi) = a\vartheta \sin(\varepsilon_i + \lambda_i) , \end{aligned} \tag{97}$$

where

$$\varepsilon_i = \Omega\left(i + \tfrac{1}{2}\right) + \varphi ; \quad \lambda_i = \Omega\left(1 + \frac{\bar{x}_i}{k}\right).\frac{1}{4} ; \quad \Omega = \omega\vartheta . \tag{98}$$

Let us suppose for simplicity's sake that a constant value is encoded in the PDM output of the multiplicator which is connected to the input of the interpolator circuit from Fig. 8. As a consequence of the pulse shifts δ_i^+ and δ_i^- an error δ_i in determining the sampling instant position Θ_i will appear. The errors δ_i^+, δ_i^-, δ_i cause a noisy output $w(t)$. Assuming a low noise level, we can neglect the influence of small deviations from equidistance of Θ_i synchronisation pulses on interpolation circuit dynamics and treat the noise to a first approximation as caused by the false determination of mean values of only the large signal inputs to the first integrator of Fig. 8. These are two: the signal $\tilde{w}(t)$ and the feedback from $w(t)$ (noise neglected).

With $A = 1$ in (51) and (53) we can for $w(t) = \text{constant} = w_0$ take $F(p)/G(p) = C/\vartheta$ as $\alpha_m = \beta_m = 1$ according to (53) and (69). Then

$$i = \frac{C}{\vartheta} w_0 . \tag{99}$$

Further, respecting (57), we find the equivalent value of the noise signal

$$\Delta w_i = -\frac{1}{\vartheta}\int_{\Theta_i}^{\Theta_{i+1}} [w_0 + k\,\tilde{w}(t)]\,\mathrm{d}t . \tag{100}$$

For $\tilde{w}(t)$ of the form of Fig. 6 for a constant $\bar{x}_i = x_0$ and $\bar{y}_i = y_0$ and respecting

$$w_0 = -x_0 y_0$$

we obtain

$$\Delta w_i = \frac{k}{\vartheta} y_0 \left[(\delta_{i+1} - \delta_i) \left(1 + \frac{x_0}{k} \right) + 2(\delta_i^+ - \delta_i^-) \right]. \tag{101}$$

Now an algorithm has to be found, determining Θ_i from measured values τ_i, that is, determining δ_i from values $(\delta_i^+ + \delta_i^-)/2$ gained by comparing τ_i with equidistant time pulses separated by an interval ϑ.

From (97) we find

$$\begin{cases} \delta_i^+ + \delta_i^- = 2a\vartheta \sin \varepsilon_i \cos \lambda \\ \delta_i^+ - \delta_i^- = -2a\vartheta \cos \varepsilon_i \sin \lambda \end{cases} \tag{102}$$

where

$$\lambda = \frac{\Omega}{4} \left(1 + \frac{x_0}{k} \right).$$

The algorithm determining for δ_i has to show a good stability and quick response, thus the choice of a response of a finite number of steps is optimal. We thus choose

$$\delta_{i+1} = \sum_{k=0} b_k \Delta^k (\delta_i^+ + \delta_i^-), \tag{103}$$

where the symbol Δ^k denotes the kth difference. Substituting (102) and (103) into (101) then leads to the result

$$\frac{\Delta w_i}{4aky_0} = -\sin \lambda \cos \varepsilon_i + \frac{4\lambda}{\Omega} \sin \frac{\Omega}{2} \cos \lambda \sum_{k=0} 2^k b_k \sin^k \frac{\Omega}{2} \sin \left[\varepsilon_i - \frac{k+1}{2} (\Omega - \pi) \right]. \tag{104}$$

Now we wish to have Δw_i as small as possible for a maximal range of Ω. For $\Omega = 0$ we hawe $\lambda = 0$ and $\Delta w_i = 0$ and we demand

$$\frac{\mathrm{d}\, \Delta w_i}{\mathrm{d}\Omega} = 0 \quad \text{and} \quad \frac{\mathrm{d}^2 \Delta w_i}{\mathrm{d}\Omega^2} = 0$$

which leads to conditions

$$b_0 = \tfrac{1}{2} \quad \text{and} \quad b_1 = \tfrac{1}{4}. \tag{105}$$

All algorithms (103), satisfying this condition, can be written in the form

$$\delta_i = \frac{1}{4} \left[\delta_i^+ + \delta_{i-1}^+ + \delta_i^- + \delta_{i-1}^- - \Delta^2 \sum_{k=0} a_k \Delta^k (\delta_i^+ + \delta_i^-) \right], \tag{106}$$

where the a_k have to satisfy the condition

$$\sum_{k=0} a_k = 1.$$

Using (106) in (101) leads to

$$\frac{\Delta w_i}{4aky_0} = \cos\varepsilon_i\left(\lambda\cos\lambda\frac{\sin\Omega}{\Omega} - \sin\lambda\right) + \frac{4\lambda}{\Omega}\sin^3\frac{\Omega}{2}\cos\lambda\sum_{k=0}2^k a_k\sin^k\frac{\Omega}{2}\sin\left[\varepsilon_i - \right.$$

$$\left. - \frac{k+1}{2}(\Omega - \pi)\right]. \tag{107}$$

To the simplest transfer function satisfying (105)

$$\delta_{i+1} = \tfrac{1}{4}[3(\delta_i^+ + \delta_i^-) - (\delta_{i-1}^+ + \delta_{i-1}^-)] \tag{108}$$

corresponds $a_0 = 1$ and

$$\frac{\Delta w_i}{4aky_0} = \cos\varepsilon_i\left(\lambda\cos\lambda\frac{\sin\Omega}{\Omega} - \sin\lambda\right) + \frac{4\lambda}{\Omega}\sin^3\frac{\Omega}{2}\cos\lambda\cos\left(\varepsilon_i - \frac{\Omega}{2}\right). \tag{109}$$

The vanishing of the first two derivatives of Ω is equivalent to the vanishing of the first two derivatives of the pulse shift $\sigma(t)$; thus with this simplest algorithm, neither a constant error in tape velocity, nor constant acceleration of the tape causes any error in the reproduced signal. This is a very important quality, achievable with PDM, which substantially simplifies the design of mechanical blocks.

λ in (107) is a function of x_0 as well as Ω. It is not possible to suppress higher derivatives of Ω than the second for all values of x_0. But the a_k values can be chosen in such a way that the influence of x_0 is held to minimum.

Studying the expression

$$\kappa\lambda\cos\lambda - \sin\lambda \tag{110}$$

we can find for a given $\lambda_{max} = (1 + 1/k)\,\Omega/4$ by series expansions an optimal $\kappa = f(\lambda_{max}) = f(\Omega)$ for which $|\kappa\lambda\cos\lambda - \sin\lambda|_{max}$ on the interval $0 \leqq \lambda \leqq \lambda_{max}$ is minimal.

The first terms of the series are

$$\kappa = 1 + \frac{\lambda_m^2}{4} + \frac{17}{240}\lambda_m^4 + \frac{433}{22\,400}\lambda_m^6. \tag{111}$$

Equation (107) then may be written

$$\frac{\Delta w_i}{4aky_0} = \cos\varepsilon_i(\kappa\lambda\cos\lambda - \sin\lambda) + \tag{112}$$

$$+ \frac{\lambda}{\Omega}\cos\lambda\left\{(\sin\Omega - \kappa\Omega)\cos\varepsilon_i + 4\sin^3\frac{\Omega}{2}\sum 2^k a_k\sin^k\frac{\Omega}{2}\sin\left[\varepsilon_i - \frac{k+1}{2}(\Omega - \pi)\right]\right\}.$$

The first term expresses the minimum possible disturbance with any choice of a_k. The second term can be held arbitrarily low by an approximate choice of a_k. The most reasonable demand is to keep the second term to zero for some important disturbing frequency, for instance the perforation frequency or gear tooth frequency.

For this it is necessary to choose

$$a_2 = 1 - (1 + 2\cos\Omega_0)\, q\,,$$

$$a_1 = -4\sin^2\frac{\Omega_0}{2} + q\left(1 + 4\sin\frac{\Omega_0}{2}\sin\tfrac{3}{2}\Omega_0\right), \tag{113}$$

$$a_0 = 1 - a_1 - a_2\,,$$

where

$$q = \frac{\kappa\Omega_0 - \sin\Omega_0}{4\sin\Omega\,\sin^2(\Omega_0/2)},$$

and κ_0 designates the value of κ for the frequency Ω_0 for which the noise has to be minimized.

For small values of $\lambda_{\max}$ ($\lambda_{\max} < \frac{1}{2}$) the minimized noise corresponding to the first term in (112) can be estimated as

$$\Delta w_i = aky_0 \cdot \frac{\lambda_m^3}{3} = \frac{ay_0k(1 + k^{-1})^3}{192}\,\Omega^3 = y_0 \cdot \vartheta^2\sigma''(t) \cdot \frac{k(1 + k^{-1})^3}{192}\,. \tag{114}$$

Thus, the influence of velocity changes can be suppressed very strongly by an appropriate synchronisation algorithm. The first derivative of $\sigma(t)$ is proportional to the relative tape velocity errors in writing (Δv_w) and reading (Δv_r)

$$\sigma'(t) = \frac{\Delta v_w + \Delta v_r}{v}\,.$$

Thus, a velocity variation of 1% amplitude in reading or writing, that is $\Delta v/v = a\vartheta\Omega\sin(\omega t + \varphi)$, $a\vartheta\omega = a\Omega = 10^{-2}$ may cause only a noise (for $k = 1{\cdot}25$) $3{\cdot}7 \cdot 10^{-4}\,\Omega^2$ of full scale. This is a negligible value for all values of Ω, for which this estimation is valid, that is, for $\Omega < 1$, $\omega < 1/\vartheta$ which corresponds to velocity variations with frequencies close to half the sampling frequency.

It is interesting to note that the tape velocity noise supression obtainable with the described synchronisation algorithms is comparable with that obtained with Θ_i synchronisation pulses taken from an auxiliary track. In the latter case

$$\delta_i = a\vartheta\sin(\omega\Theta_i + \varphi) = a\vartheta\sin\left(\varepsilon_i - \frac{\Omega}{2}\right), \tag{115}$$

$$\delta_{i+1} - \delta_i = 2a\vartheta\cos\varepsilon_i\sin\frac{\Omega}{2}\,,$$

and

$$\frac{\Delta w_i}{4aky_0} = \left(\lambda\,\frac{\sin\dfrac{\Omega}{2}}{\dfrac{\Omega}{2}} - \sin\lambda\right)\cos\varepsilon_i\,, \tag{116}$$

the first term of series expansion being

$$(117)\qquad \frac{\Delta w_i}{4aky_0} \doteq \left(\frac{\lambda^3}{6} - \frac{\lambda\Omega^2}{24}\right)\cos\varepsilon_i = \frac{\Omega^3}{384}\left(3 + \frac{x_0}{k}\right)\left(\frac{x_0^2}{k^2} - 1\right)\cos\varepsilon_i$$

yielding a maximum error for $x_0/k = 2/\sqrt{3} - 1$

$$(118)\qquad \Delta w_i = aky_0\frac{\Omega^3}{54}\sqrt{3} = 4{\cdot}012\,.\,10^{-2}ay_0\Omega^3\,,$$

whereas (114) yields for the same value of $k = 1{\cdot}25$

$$(119)\qquad \Delta w_i = 3{\cdot}7\,.\,10^{-2}ay_0\Omega^3\,.$$

For the simplest algorithm (108) the error estimation is

$$(120)\quad \Delta w_i = \frac{aky_0}{48}\left(1 + \frac{1}{k}\right)\left[\left(1 + \frac{1}{k}\right)^2 - 16\right]\Omega^3 = 0{\cdot}598ay_0\Omega^3 \quad \text{for} \quad k = 1{\cdot}25$$

and would be satisfactory only if the velocity error were low or slow. A PDM signal based on a saw-tooth coding seems to have the advantage of carrying the synchronisation track in itself – one of the polarity changes of the PDM corresponds to the steep front of the saw-tooth which has to be separated from the sampling instant by a small fixed interval.

But in spite of this an analysis quite similar to the above indicates that the noise situation is much worse in this case. From Fig. 7 and (100) we can derive

$$(121)\qquad \Delta w_i = -\frac{k}{\vartheta}y_0\left[\delta_{i+1} + \delta_i + \frac{x_0}{k}(\delta_{i+1} - \delta_i) - 2\delta_i^+\right].$$

Using for δ_i (114) and for δ_i^+

$$(122)\qquad \delta_i^+ = \sin\left(\varepsilon_i + \frac{\Omega x_0}{2k}\right)$$

we obtain

$$(123)\quad \frac{\Delta w_i}{2aky_0} = \sin\varepsilon_i\left(\cos\frac{\Omega x_0}{2k} - \cos\frac{\Omega}{2}\right) + \cos\varepsilon_i\left(\sin\frac{\Omega x_0}{2k} - \frac{x_0}{k}\sin\frac{\Omega}{2}\right).$$

Maximum of noise appears for $x_0 = 0$. Thus for the maximum amplitude of Δw_i we have

$$(124)\qquad \Delta w_i = 4aky_0\sin^2\frac{\Omega}{4} = \tfrac{1}{4}aky_0\Omega^2\,.$$

That is, of course, much worse than all preceding cases and indicates sensitivity to constant acceleration. Therefore the advantages of a triangular waveform are demonstrated once more.

Finally, it may be stressed that all the advantages of a triangular coding waveform shown, that is

a) low gain requirement for the generating integrator
b) low quality requirements for the SH circuit in coding and multiplication applications
c) possibility of high suppression of influence of tape velocity variations without use of an auxiliary synchronisation track

may be used simultaneously in practice as the influence of waveform imperfectness and the sampling-holding action imperfectness on the intrinsic synchronisation information content of the PDM signal is only of secondary importance. This can be shown by detailed analysis which, however, is beyond the scope of the paper.

APPENDIX

Triangular waveform generation

Fig. 15 shows the basic circuit structure used in MUSA for the generation of the triangular waveform.

In Fig. 16 are indicated the waveforms in some points of the circuitry of Fig. 15.

The rectangular output of A_1 and A_2 is integrated by A_3. In the moment when the sum of voltages in points 1 and 2 is zero, a polarity change in the output of A_4 is effected. The output of

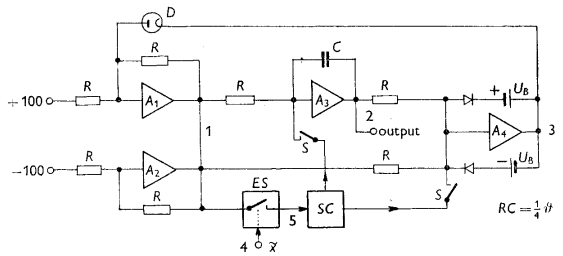

Fig. 15. Triangular waveform generator circuitry.

A_4 by means of the diode D controls the pair of inverters A_1 and A_2. If the output of A_4 is negative, A_1 is blocked and A_2 is working. If the output of A_4 is positive, the diode D is closed and A_1 is working, maintaining —100 V on its output. Thus A_2 is blocked by a great negative voltage on its grid. The polarity change of output of A_4 thus effects a polarity change in the output voltage of A_1 and A_2, causing, in this way, an inversion of the slope of the triangular wave. We can see that the accuracy of peak amplitudes of the triangular voltage is given mainly by resistor accuracy and zero drifts of A_1, A_2, A_4, if the gain of A_1 and A_2 is sufficient. The transients due to the switching of A_1 and A_2 cause of course some slight distortion of the peaks of the triangular waveform. But only 80% peak amplitude of the coding waveform is actually used for coding with $k = 1.25$. Thus the peak distortion is harmless.

The switches S are open when the triangular waveform is used for coding; they are closed when the scheme is used as a generator of synchronising Θ_i pulses. These are derived from the negative edges of A_4 output. As a measure of the quantity $\delta_i - \frac{1}{2}(\delta_i^+ + \delta_i^-)$ the mean value of the output of the electronic switch ES is used. This switch is closed only for the positive polarity of $\tilde{x}(t)$. The

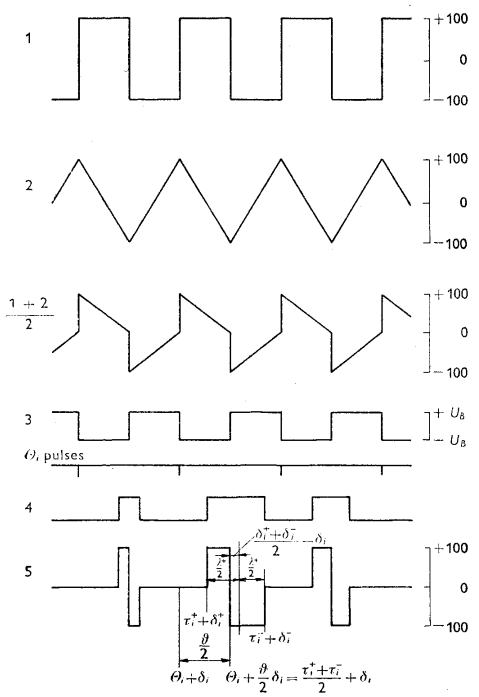

Fig. 16. Waveforms of the coding waveform generator.

synchronisation controller SC influences the amplitude and the slope of the triangular waveform in order to secure the necessary transfer function between $(\delta_i^+ + \delta_i^-)$ and δ_i.

(Received June 13th, 1964.)

REFERENCES

[1] Brooks F. E., Smith H. W.: A Computer for Correlation Functions. Review of Scientific Instruments 23 (1952), No 3, pp. 121—126.

[2] Holmes J. N., Dukes M. A.: A Speech Waveform Correlator with Magnetic Tape Delay and Electronic Multiplication. Proc. IEE *101* (1954), No 72, pp. 225—237 (Radiosection Paper No 1639)

[3] Бабурин В М.: Коррелограф-прибор для вычисления корреляционых функций низкочастотных процессов. Сборник: Применение вычислительной техники для автоматизации производства. Машгиз, Москва 1961.

[4] Новиков Ю. В.: Магнитный коррелограф. Серия „Приборы и стенды", Изд. Института тех. -экон. информации АН СССР, Москва 1956.

[5] Lee I. W., Cheatham T. P., Wiesner J. B.: Application of Correlation Analysis to the Detection of Periodic Signals in Noise. Proc. IRE *38* (1950), No 10, pp. 1165—1172.

[6] Levin M. J., Reintjes F. J.: A Five-Channel Electronic Analog Correlator. Proc. of National Electronic Conference *8* (1952), pp. 647—656.

[7] Reintjes F. J.: An Analogue Electronic Correlator. Proc. of National Electr. Conference *7* (1951), pp. 390—400.

[8] Šilhánek: Užití analogových počítačů v regulaci a automatizaci. Publikace: Elektronické analogové počítače, Tesla Pardubice 1960.

[9] Maxwell: Development of a Portable Magnetic Tape Recorder for Precision Data Recording. IRE Convention Record (1955), Part 10, p. 97.

[10] Newhouse: Compound Modulation-Method of Recording Data on Magnetic Tape. IRE Convention Record (1955), Part 10, p. 86.

[11] Reukauf: Simulate Transport Lags with Magnetic Tape. Control Engineering *4* (1957), No 6, pp. 145—147.

[12] Blandhol, E. Balchen J. G.: On the Experimental Determination of Statistical Properties of Signals and Disturbances in Automatic Control Systems. Trans. IFAC Congress, Moscow 1960, vol. 2, pp. 788—796.

[13] Blandhol, Hestrik, Mohus: A Description of the Statistical Computer "ISAC". Automatic Control Laboratory, Norwegian Institute of Technology, vol. 1 (Nov. 1959) and vol. 2 (Dec. 1960).

[14] Krýže J.: A Universal Statistical Analyser. Trans. IFAC Congress, Basel 1963.

[15] Krýže J.: MUSA-6 — ein universeller statistischer Analysator. Zeitschrift für Messen, Steuern, Regeln 6 (1963), No 7, pp. 286—298 and No 9, pp. 386—391.

Metody pro zapamatování a zpracování analogových signálů použité ve stroji MUSA-6

JIŘÍ KRÝŽE

Práce popisuje algoritmy pro zapamatování a zpracování analogových signálů použité ve stroji MUSA-6, jenž je určen zejména pro vyhodnocování náhodných procesů. Algoritmy jsou důsledně založeny na časově diskrétní reprezentaci signálů. Vhodnou volbou transformací ze spojitého signálu na diskrétní je využito maximum možností, které uvedená metoda skýtá, a dosaženo necitlivosti k různým nedokonalostem elektronických i mechanických funkčních bloků stroje. Je uveden zobecněný matematický rozbor použitých metod, jenž může nalézt uplatnění zejména tam, kde se používá šířkové pulsní modulace pro přesný magnetofonový záznam analogových signálů.

Inž. Jiří Krýže, CSc., Ústav teorie informace a automatizace ČSAV, Českomalínská 25, Praha 6.